

Received January 25, 2021, accepted February 4, 2021, date of publication February 11, 2021, date of current version February 24, 2021.

Digital Object Identifier 10.1109/ACCESS.2021.3058647

# Beam-Steerable Passive Transmitarray Optimized Based on an Adjacent Algorithm

EUIHO SHIN<sup>1</sup>, (Student Member, IEEE), AND JUNGSEUK OH<sup>2</sup>, (Senior Member, IEEE)

<sup>1</sup>Institute of New Media and Communications, Seoul National University, Seoul 08826, South Korea

<sup>2</sup>Department of Electrical and Computer Engineering, Seoul National University, Seoul 08826, South Korea

Corresponding author: Jungseuk Oh (jungseuk@snu.ac.kr)

This work was supported in part by the Creative-Pioneering Researchers Program of Seoul National University (SNU), and in part by Institute of Information and Communications Technology Planning and Evaluation (IITP) grant by the Korean Government through Ministry of Science and ICT (MSIT) (Millimeter-wave Metasurface-based Dual-band Beamforming Antenna-on-Package Technology for 5G Smartphone) under Grant 2020-0-00858.

**ABSTRACT** This paper presents a novel adjacent algorithm for the design of a beam-steerable passive transmitarray (TA) antenna. Even if the beam of a feed antenna is steering by varying the phase offset of the antenna array forming the feed antenna, the existing passive TA, which improves the gain only in the boresight direction, cannot improve the gain in all directions in which the beam is steering. To minimize the difference in the phase shift between different phase offsets by adjusting the reference phase instead of searching the entire space made up of the reference phase of each phase offset, an adjacent algorithm to change the reference phase with an adjacent phase that minimizes the objective function was adopted. This strategy improved the  $O(n^{k-1})$  algorithm to a linear algorithm of  $O(n)$ . It was also experimentally shown that optimization using the adjacent algorithm did not change the final result regardless of the initial value. Weighing the magnitude of the electric field (E field), the average optimized phase shift was obtained to determine the phase shift of the passive TA unit cell. Simulation of a TA consisting of an effective simple medium with a thickness of 2.5 mm reflecting the previously determined phase shift showed that the gain was improved by less than 1 dB when the phase offset was  $0^\circ$  and by more than 1 dB when the phase offset was  $75^\circ$ .

**INDEX TERMS** 5G, adjacent algorithm, optimization, transmitarray.

## I. INTRODUCTION

5G communication technology, currently a hot topic, is expected to encompass ultra-reliable and low-latency communication (URLLC), enhanced mobile broadband (eMBB), and massive-machine-type communications (MMTC) through its use of the millimeter-wave band. However, considering that signals at millimeter-wave bands are subject to high path loss due to their extreme straightness, a high antenna gain is required to compensate for the loss, though this narrows the beam width. Therefore, a beam-steering feature has become an essential and important feature for 5G antennas given their high antenna gain.

Lenses have been widely used to achieve both of the aforementioned characteristics. First, as the lens compensates for the phases of the incident wave, the desired beam can be

created, and a gain enhancement can be achieved. A dielectric lens was used to transform the desired wave form according to its curved surface, similarly to an optical lens [1], [2]. An antenna-filter-antenna (AFA) lens, used here as a phase changing lens, has a planar shape, in contrast to a dielectric lens. Each unit cell that comprises the AFA consists of two antennas and filters, which are used to resonate with electromagnetic waves to receive and radiate waves and to change the phase of the incident wave [3]. Compared to a dielectric lens, the AFA is advantageous because it has fewer process errors, also offering a geometrical advantage given its planar structure. A frequency-selective surface, consisting of metal layers and substrates, has recently been employed as a unit cell in lenses for beam forming [4], [5]. It has advantages such as a simple structure, the ability to derive an accurate filter response, and miniaturization. Nevertheless, the conventional passive transmitarray (TA) or lens was only designed to enhance the gain in the boresight

The associate editor coordinating the review of this manuscript and approving it for publication was Emanuele Crisostomi<sup>1</sup>.

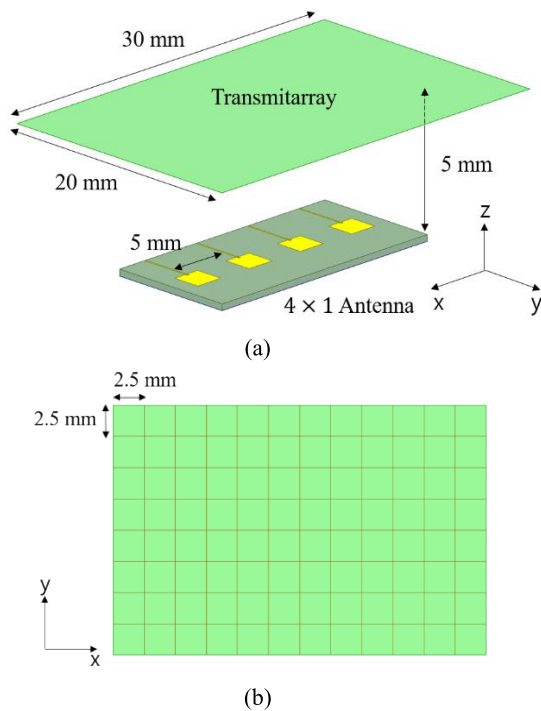


FIGURE 1. (a) Total structure of the TA antenna, and (b) a TA consisting of 96 unit cells.

direction [6]–[9]. If unit cells are arranged using the phase distribution on a TA based on the beam of the feed antenna in the direction of the boresight, the gain improvement is smaller in the remaining directions apart from the boresight direction [7], [10]. Some studies have shown different unit cell layouts that are robust to beam steering in a feed antenna to compensate for the gain reduction [10], but different beam-steering angles were not considered.

The beam-steering feature can be achieved by employing active components or active materials such as varactors, pin diodes, and liquid crystal in antennas [11]–[13], especially in reflectarray (RA) antennas and TA antennas for beam steering. This is achieved by changing the characteristics of the component or material without changing the structure by applying power [14]–[17]. However, this is also associated with a high side lobe level and does not offer much of a gain improvement. Moreover, liquid crystal is a liquid-state substance, which makes it difficult to process a RA or TA even in simple structures. In order to change the properties of the RA or TA and to steer the beam, power must be applied regardless of the active components or active materials used. As frequency band used increases, devices become smaller, meaning that the batteries used lack space to power the active component or bias the active material. In contrast, passive TAs have been widely used, are relatively easy to manufacture, and require no additional power. [18]

In this paper, we propose an optimization methodology by which a passive TA stably increases the gain in the beam-steering angle of the main beam of a feed antenna in various

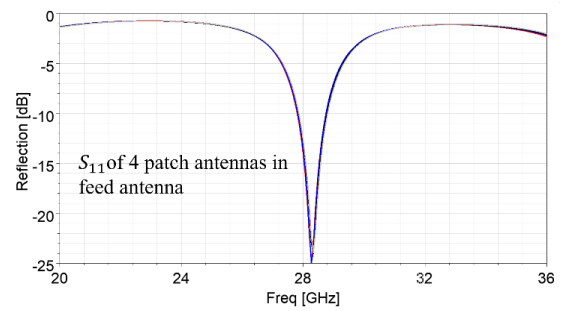


FIGURE 2. Reflection of four patch antennas in a feed antenna.

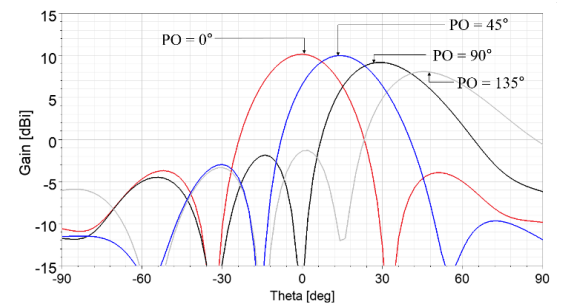


FIGURE 3. Beam steering from a feed antenna when PO is 0°, 45°, 90°, and 135°.

directions and a potential design of optimized TA. An area with a large magnitude of the electric field (E field) has more influence on beam forming; therefore, the phase as well as the magnitude of the E field are considered to optimize the phase shift arrangement of the unit cells. However, attempting to find the optimal arrangement by exploring all possible cases leads to an impractical optimization algorithm with  $O(n^2)$  or higher time complexity, where  $n$  is the number of phases to be explored depending on the rate at which the phase is updated during the optimization process [19]. Therefore, we propose an adjacent algorithm by which the optimal arrangement can be reached within linear time.

In Section II, the reason why optimization is needed to design a beam-steerable passive TA is presented. In Section III, the optimization problem is defined and the novel methodology used here is proposed and discussed. Additionally, the passive TA is designed and simulated in Section IV. In Section V, the conclusion is presented.

## II. NECESSITY OF OPTIMIZATION

### A. SIMULATION RESULT

This section presents the feature of the TA antenna used for optimization and the simulation result. Fig. 1 (a) shows the overall structure of the TA antenna, which consists of a  $4 \times 1$  patch antenna and the passive TA.

Fig. 2 shows that the  $S_{11}$  of the four patch antennas forming the feed antenna is  $-25$  dB at 28 GHz, which means that the target frequency of the feed antenna is 28 GHz. The distance between each patch antenna in the feed antenna is 5 mm ( $0.5 \lambda_0$ ). The distance between the feed antenna and

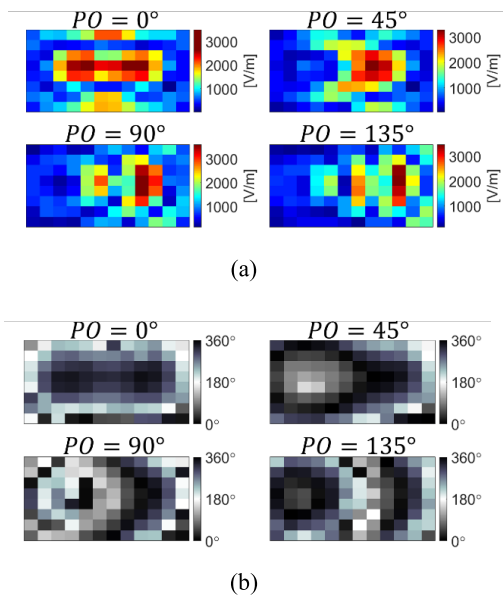


FIGURE 4. (a) Captured magnitude and (b) phase of the E field on each center of the unit cell on the TA.

the TA is 5 mm ( $0.5 \lambda_0$ ), i.e., as thick as a mobile phone, and the size of the TA is 30 mm  $\times$  20 mm ( $3\lambda_0 \times 2\lambda_0$ ). Fig. 1 (b) shows that the size of a unit cell is 2.5 mm  $\times$  2.5 mm ( $0.25\lambda_0 \times 0.25\lambda_0$ ) and that the passive TA consists of 96 unit cells. The beam radiated from the  $4 \times 1$  patch antenna is steered to  $\theta = 0^\circ, 14.5^\circ, 30^\circ,$  and  $48.6^\circ$  based on antenna array theory when the phase offset (PO) is  $0^\circ, 45^\circ, 90^\circ,$  and  $135^\circ$ , respectively, as depicted in Fig. 3 [20]. When the PO is  $0^\circ$ , the gain of the feed antenna is 10 dB, and the gain decreases as the PO increases. In this structure, the phase and magnitude of the E field at each center of the unit cell were simulated and captured using ANSYS HFSS to optimize the unit cell characteristics of the TA and to arrange the unit cells; these results are shown using MATLAB in Fig. 4. This depicts a capture of the phase and magnitude in the absence of a TA. In the simulation results, the unit cell with a high magnitude of the E field moves in the positive direction on the x-axis and the concentric circle shape in the captured phase of the E field moves in the negative direction on the x-axis as the PO of the feed antenna increases, consistent with the beam-steering direction shown in Fig. 3.

**B. PHASE SHIFT DIFFERENCE BETWEEN DIFFERENT POs**

To enhance the gain in the direction of the main beam of the feed antenna, the proper phase shifts of the unit cells must be calculated. Fig. 5 (a) presents the desired phase above the TA to improve the gain toward the direction of the main beam of the feed antenna according to the PO, which is calculated based on antenna array theory. Because the magnitude of the phase progression is  $kdsin\theta\cos\phi$  [20], where  $k$  is the wave number,  $d$  is the distance between the unit cells, and  $\phi$  is  $0^\circ$ , the phase progression increases as  $\theta$  grows, which is consistent with Fig. 5 (a). In order to obtain the phase shift

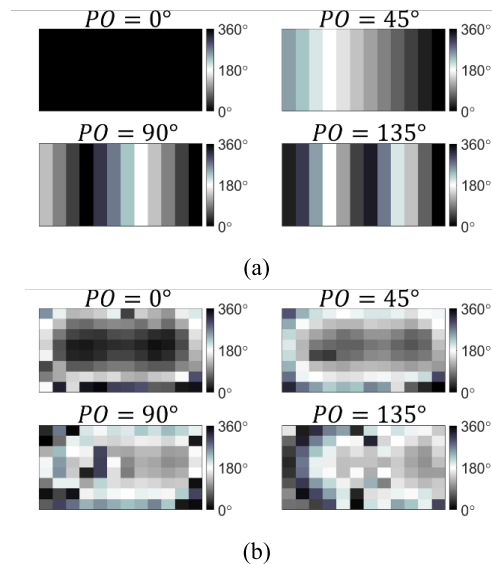


FIGURE 5. (a) Desired phase for a gain improvement in the direction of the main beam according to the PO and (b) phase shift of the unit cells to achieve the desired phase in Fig. 5 (a).

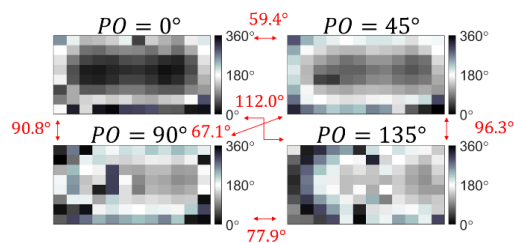


FIGURE 6. Differences in the phase shifts between two different POs calculated using (1).

of the unit cell, the difference between the phase in Fig. 5 (a) and Fig. 4 (b) must be obtained, and by arranging the unit cell with the phase shift obtained as such, the gain can be increased by forming a beam with a wave front perpendicular to the direction of the wave propagation.

The 2-norm difference in the phase shifts of the unit cells between the  $n$ -th PO and the  $m$ -th PO,  $D_{mn}$ , was calculated using (1).

$$D_{mn} = \sqrt{\frac{\sum_{i=1}^{12} \sum_{j=1}^8 \text{mod}(|P_{n,ij} - P_{m,ij}|, 360^\circ)^2}{12 \times 8}} \quad (1)$$

Here,  $P_{n,ij}$  is the phase shift of the  $i$ -th column of the  $j$ -th row unit cell in the  $n$ -th PO and  $\text{mod}$  is the modular operator that returns the remainder divided by a given number. Equation (1) serves as a measure of how much of a difference there is between the two POs, and it is used here to indicate that the difference has decreased due to optimization. The difference was at least  $59^\circ$  and at most  $112^\circ$ , as shown in Fig. 6. Because the differences between the POs are too large to use one of these collections of phase shifts as a passive TA at different

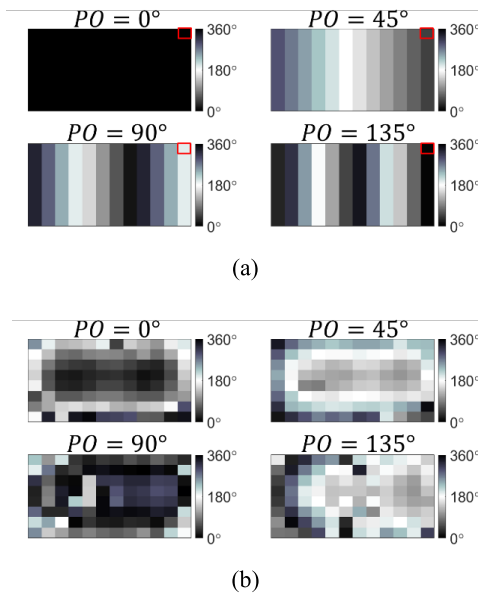


**FIGURE 7.** (a) Desired phase of the TA and (b) calculated phase shift of a unit cell with different reference phase combinations (red boxes in (a) mean reference phases, which are 0°, 45°, 90°, and 135°, respectively).

beam-steering angles, optimization is needed to minimize the difference calculated by (1).

### III. OPTIMIZATION METHODOLOGY

#### A. OPTIMIZATION PROBLEM DEFINITION

In Fig. 5 (a), the desired phase of the unit cell which is located in the first row of the last column is referred to as the ‘reference phase’, and these are all set to 0° for all POs. According to antenna array theory [20], only the phase progression and distance between the elements affect the antenna pattern, meaning that the gain improvement is independent of the value of the reference phase and that the phase of the desired TA can be changed by varying the reference phase. Therefore, it is possible to modify the reference phases to minimize the differences in the phase shifts of the unit cells between pairwise POs. For example, as depicted in Fig. 7, despite the fact that the desired phase was calculated when the reference phases at 0°, 45°, 90°, and 135° were 0°, 45°, 193°, and 357°, respectively, they still enhance the antenna gain in a direction identical to that of the phase shift in Fig. 5 (b). With the reference phase fixed at 0° when PO is 0°, the three remaining reference phases were changed, and optimization was carried out to reduce unnecessary processes.

The optimization problem is defined as a minimization problem via (2), as shown at the bottom of the next page: where  $E_{n,ij}$  is the magnitude of the E field in the unit cell of the  $i$ -th column of the  $j$ -th row with the  $n$ -th PO and  $R_n$  is the reference phase of the  $n$ -th PO. A comparison of Fig. 5 (b) and Fig. 7 (b) shows that as the reference phase changes, the phase shift changes and the difference between the phase shift of the pairwise POs changes. Taking this into account,

#### Adjacent algorithm

```

Obj( $R_n$ ) // objective function of reference phase
 $s \leftarrow 1$  // phase step = 1°
repeat
  for each  $R_n$  do
    if  $Obj(R_n) > Obj(R_n + s)$  or  $Obj(R_n) > Obj(R_n - s)$  do
      if  $Obj(R_n) > Obj(R_n + s)$ 
        then  $R_n \leftarrow R_n + s$ 
      else if  $Obj(R_n) > Obj(R_n - s)$ 
        then  $R_n \leftarrow R_n - s$ 
      end if
    end if
  end for
until for all  $R_n$ ,  $\min(Obj(R_n), Obj(R_n + s), Obj(R_n - s)) = Obj(R_n)$ 
return all  $R_n$ 

```

**FIGURE 8.** The pseudo code of an adjacent algorithm.

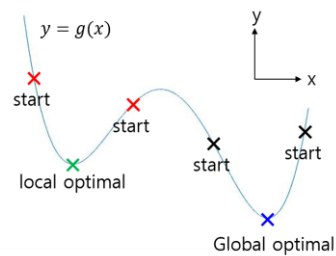


**FIGURE 9.** Global optimal value convergence according to the initial value.

the optimization problem is a problem of setting the reference phases as variables and finding the combination of reference phases that minimizes the objective function. The larger the magnitude of the E field, the greater the effect it has on the beam forming. Accordingly, weighting of the magnitude of the E field in the objective function is conducted to prioritize the optimizing of the unit cell with a larger magnitude.

#### B. OPTIMIZATION USING ADJACENT ALGORITHM

However, if all combinations of changing the reference phases are searched to find the minimum value of the objective function, referred to as a naïve method, the time complexity is  $O(n^{k-1})$ , where  $k$  is the number of POs and  $n$  is the number of phases to be searched in each reference phase. A naïve algorithm explores all combinations of variables; therefore, multiplying by the number of cases for each variable can determine the number of combinations of all variables, which leads to cubic polynomial time complexity in this optimization problem. In order to overcome the impractical time complexity of a naïve algorithm, an adjacent algorithm, similar to a greedy algorithm, was used, which was also used in [21]. Fig. 8 presents the pseudo code of an adjacent algorithm. The adjacent algorithm undertakes optimization of each variable, in turn, until all variables are optimized. After the optimization of a single reference phase is completed, optimization for other POs begins, and this

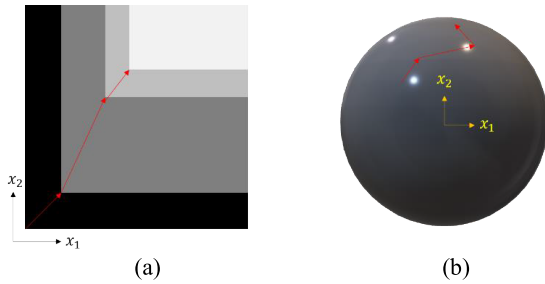


**FIGURE 10.** Visualization of the searching space and optimization process of (a) a greedy algorithm and (b) the adjacent algorithm with two variables.

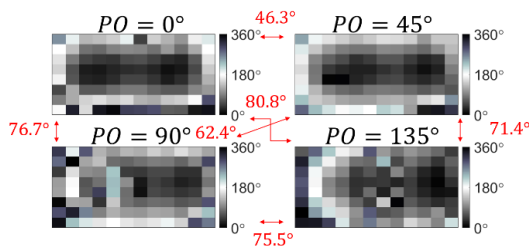


**FIGURE 11.** Optimized differences of phase shifts between two different POs.

process repeats in the same way, with the local best choices being made and the reference phase updated by a specific rate, which is 1° in this case. This process is repeated for all variables, and the number of iterations can vary depending on the problem.

However, local optimization does not always result in a global optimal and may depend on the initial value of the optimization problem. As shown in Fig. 9, the pursuit of the local optimal may or may not converge to the global optimal depending on the initial value. To demonstrate that the optimality derived by the initial value does not vary, all reference phase combinations of 10° intervals were initially taken, confirming that the resulting optimality was within 0.3% error of the global optimal derived by the naïve algorithm and that there was nearly no difference, which means this optimization problem has a greedy choice property.

The following two conditions must be satisfied to use the greedy algorithm: greedy choice property and an optimal substructure [19]. These mean that previous choices do not affect subsequent choices and that the subproblem and the original problem should have the same degree of optimality. The problem is not addressed by the greedy algorithm

because the periodic structure of the phase makes it difficult to determine the subproblem; therefore, it is impossible to differentiate between previous and subsequent choices. The problem and solution of the greedy algorithm and the adjacent algorithm with two variables can be expressed as Fig. 10 (a) and Fig. 10 (b), respectively. In the former case, the entire space to be explored can be expressed in the form of a rectangle, defining a rectangular subproblem resembling the original problem, making local best choices following the red arrows and gradually simplifying the problem. On the other hand, the latter case, i.e., the adjacent algorithm, cannot simplify the problem by defining a subproblem because the entire space made up of periodic variables is the surface of a sphere, and unlike a rectangle, it is impossible to find a spherical subproblem on the surface of the sphere. Therefore, the optimal solution can be found along the red arrow, but it does not simplify the problem to a subproblem. Therefore, the adjacent algorithm is appropriate for solving problems that only have greedy choice property like this optimization problem.

**IV. SIMULATION RESULT**

After the optimization process was complete, the difference in the phase shift became at least 46° and reached as high as 80°, and the optimized reference phases were 323°, 293°, and 249° when the PO was 45°, 90°, and 135°, respectively, as shown in Fig. 11. In Fig. 12, which shows the difference in the phase shift between the two POs in rows and columns before and after the optimization, the changes in the difference of the phase shifts between the two POs in each unit cell can be compared. In other words, Fig. 12 (a) and Fig. 12 (b) present the differences in the phase shifts between two POs in the unit cells calculated using the values in Figs. 6 and 11, respectively. In Fig. 12, therefore, by comparing the difference in the phase shift between the two POs before and after optimization, not only the mean difference, such as (1), but also the change before and after optimization of each unit cell can be observed. It was also noted that the whiter the area of a unit cell is, the closer the difference between the unit cells is to 0° and that there are more bright areas after optimization.

Compared with Fig. 4 (a), after optimization, these unit cells are more distributed in areas of greater magnitudes of the E field. It also can be inferred that the more differences between POs there are, the less bright the unit cell area is, which means that the greater the beam-steering angle,

$$\min_{R_n} \sum_{n=1}^4 \sum_{m>n}^4 \sqrt{\frac{\sum_{i=1}^{12} \sum_{j=1}^8 (E_{n,ij} - E_{m,ij}) \bmod (|(P_{n,ij} + R_n) - (P_{m,ij} + R_m)|, 360^\circ)^2}{\sum_{i=1}^{12} \sum_{j=1}^8 (E_{n,ij} - E_{m,ij})}}$$

Subject to  $0 \leq R_n < 360$  ( $n = 2, 3, 4$ ), (2)

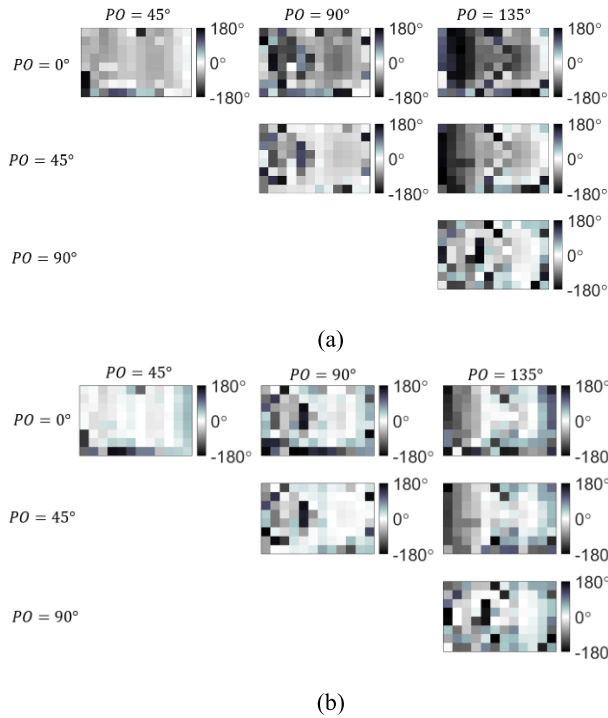


FIGURE 12. Unit cell-wise graphical comparison of differences in the phase shift: (a) before and (b) after optimization.

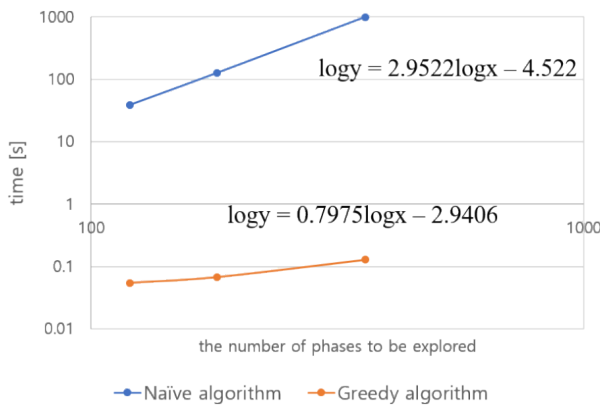


FIGURE 13. Cubic time complexity of the naïve algorithm and linear time complexity of the adjacent algorithm.

the more difficult it becomes to create a passive TA that supports various beam-steering angles by means of optimization.

The proposed algorithm has  $O(n)$  time complexity, which is considerably more practical than the  $O(n^3)$  time complexity of the naïve algorithm. Fig. 13 shows the operating time of each algorithm as a function of the log scale with the number of phases being searched. The slope of each line corresponds to the power of the polynomial of the time complexity. A result within an error range of 1.5% was derived from the naïve algorithm, while an error range of approximately 20% was derived from the adjacent algorithm, possibly due to the number of iterations. With regard to the number of

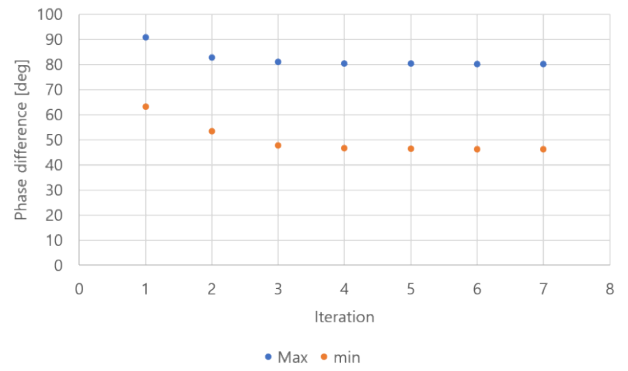


FIGURE 14. Improvement of the maximum and minimum phase difference according to the number of iterations.

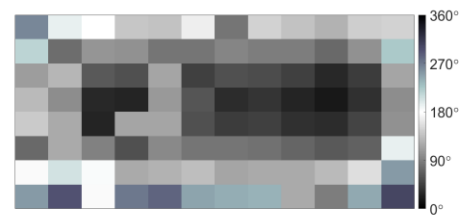


FIGURE 15. Determined phase shift of the passive TA according to the magnitude-weighted average of the optimized phase shift in Fig. 10.

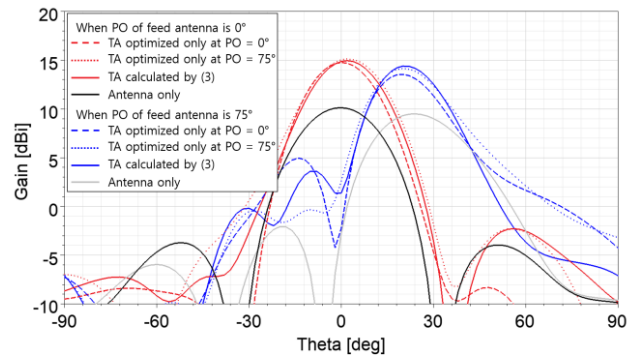


FIGURE 16. Gain improvement of less than 1 dBi after optimization when  $PO = 0^\circ$  and gain improvement of more than 1 dBi after optimization when  $PO = 75^\circ$ .

iterations needed to achieve a result identical to that of naïve algorithm, at a rate of  $1^\circ$ , it took seven iterations to obtain the optimal solution. Fig. 14 shows how the maximum and minimum values of the mean difference change with the number of iterations. After three iterations, it can be seen that both the maximum and minimum values become saturated. It took seven iterations to obtain the optimal reference phases when the rate was  $1^\circ$ . Fig. 14 presents how the maximum and minimum values of the average difference change according to the number of iterations.

The difference was fully minimized, and the phase shift property of the unit cell should be specified using the optimized results to design a passive TA. The higher the magnitude of the unit cell becomes, the greater the effect the unit

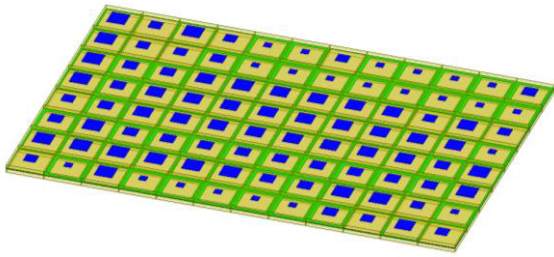


FIGURE 17. The potential design of the optimized TA.

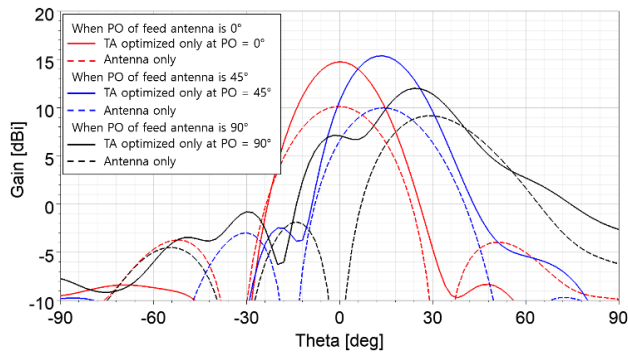


FIGURE 18. Decreasing the gain improvement of TAs and increasing the gap between the beam-steering angle of the feed antenna alone and with the TA as the PO increases.

cell has on the gain improvement. Hence, the phase shift of the passive TA was determined to be the magnitude-weighted average of the optimized phase shift according to (3), and the determined phase shift of each unit cell is depicted in Fig. 15.

$$P_{opt,ij} = \frac{\sum_{k=1}^n E_{k,ij} P_{k,ij}}{\sum_{k=1}^n E_{k,ij}} \quad (3)$$

At this stage, based on the determined phase shift of the passive TA, the gain improvements of passive TA in various directions are verified by simulations. However, for simulations using unit cells, designing the unit cells requires a considerable amount of time, and errors can occur because each unit cell has different transmission losses. Therefore, an effective simple medium was used instead of unit cells to save time and to ensure that the gains of various beam-steering directions are actually improved [10]. After optimizing the POs of the feed antenna at  $0^\circ$  and  $75^\circ$ , the phase change of the passive TA was determined by (3), and the gain improvement of the optimized case was ensured using an effective medium instead of unit cells by ANSYS HFSS. The thickness of the effective medium structure was selected to be 2.5 mm and the lateral dimension of the unit cell was 2.5 mm. The TA design follows the procedure described in the literature [10]. The potential design of TA using unit cells based on the state of art is depicted in Figure 17.

As a result, as shown in Fig. 16, when the PO of the feed antenna was  $0^\circ$ , there was a gain improvement of less

than 1 dBi compared to when the TA was optimized only at  $0^\circ$  and  $75^\circ$  and there was a gain improvement of 5 dBi compare to when using the feed antenna alone. In addition, there was a gain improvement greater than 1 dBi compared to the TA optimized at  $0^\circ$  with a beam-steering angle of about  $23^\circ$  at a PO of  $75^\circ$ , and the gain improvement was 5 dBi compared to when only the feed antenna was used. In order to compare this with an account of gain improvement efficiency in the literature [10], the relationship between the aperture efficiency and the antenna gain was used [20]. The calculated gain improvement efficiency in one earlier study [10] was 0.0005, while that in the present paper is 0.0167, representing an improvement of approximately 27 times.

However, if the beam-steering angle is greater than approximately  $30^\circ$ , the lit region is limited to only a side portion of the TA, and desired phase shown in Fig. 7 (a) is calculated assuming that the magnitudes of the E field are all constant above the area where the TA is supposed to be. Thus, the gain improvement due to the TA is reduced and the beam-steering angle is slightly different from the desired direction of beam steering, as depicted in Fig. 17. If the desired phase is calculated considering the magnitude of the E field, optimization will be efficient even at POs with beam-steering angles greater than  $30^\circ$ .

## V. CONCLUSION

In this paper, a novel optimization method of the phase shift of unit cells in a beam-steerable passive TA antenna at various angles is introduced. The approach employs an adjacent algorithm considering that the desired phase is unrelated to the reference phases. The proposed method caused the process of optimization to be more efficient and more practical. It was also verified in a simulation with an effective medium that there were gain improvements of a passive TA with the determined phase shifts in various directions. This advance will simplify commercialization efforts due to its ease of production, the lower cost, and the lack of required power. Even if a reconfigurable TA must be used, the minimized difference between the POs by the proposed algorithm will even allow a small tunable range of active unit cells to be sufficient to steer the beam.

## REFERENCES

- [1] B. Chantraine-Bares, R. Sauleau, L. L. Coq, and K. Mahdjoubi, "A new accurate design method for millimeter-wave homogeneous dielectric substrate lens antennas of arbitrary shape," *IEEE Trans. Antennas Propag.*, vol. 53, no. 3, pp. 1069–1082, Mar. 2005.
- [2] M. G. M. V. Silveirinha and C. A. Fernandes, "Shaped double-shell dielectric lenses for wireless millimeter wave communications," in *IEEE Antennas Propag. Soc. Int. Symp. Transmitting Waves Prog. Next Millennium. Dig. Held Conjoint, USNC/URSI Nat. Radio Sci. Meeting*, vol. 3, Dec. 2000, pp. 1674–1677.
- [3] A. Abbaspour-Tamijani, L. Zhang, and H. K. Pan, "Enhancing the directivity of phased array antennas using lens-arrays," *Prog. Electromagn. Res. M*, vol. 29, pp. 41–64, Jan. 2013.
- [4] M. A. Al-Joumayly and N. Behdad, "A generalized method for synthesizing low-profile, band-pass frequency selective surfaces with non-resonant constituting elements," *IEEE Trans. Antennas Propag.*, vol. 58, no. 12, pp. 4033–4041, Dec. 2010.

- [5] K. Sarabandi and N. Behdad, "A frequency selective surface with miniaturized elements," *IEEE Trans. Antennas Propag.*, vol. 55, no. 5, pp. 1239–1245, May 2007.
- [6] F. Foglia Manzillo, A. Clemente, and J. L. Gonzalez-Jimenez, "High-gain D-band transmitarrays in standard PCB technology for beyond-5G communications," *IEEE Trans. Antennas Propag.*, vol. 68, no. 1, pp. 587–592, Jan. 2020.
- [7] J. Oh, "Millimeter-wave thin lens employing mixed-order elliptic filter arrays," *IEEE Trans. Antennas Propag.*, vol. 64, no. 7, pp. 3222–3227, Jul. 2016.
- [8] Q. Luo, S. Gao, M. Sobhy, X. Yang, Z.-Q. Cheng, Y.-L. Geng, and J. T. S. Sumantyo, "A hybrid design method for thin-panel transmitarray antennas," *IEEE Trans. Antennas Propag.*, vol. 67, no. 10, pp. 6473–6483, Oct. 2019.
- [9] J. Oh, "Millimeter-wave short-focus thin lens employing disparate filter arrays," *IEEE Antennas Wireless Propag. Lett.*, vol. 15, pp. 1446–1449, 2016.
- [10] Y. Kim, H. Kim, I. Yoon, and J. Oh, " $4 \times 8$  patch array-fed FR4-based transmit array antennas for affordable and reliable 5G beam steering," *IEEE Access*, vol. 7, pp. 88881–88893, 2019.
- [11] W. Hu, R. Dickie, R. Cahill, H. Gamble, Y. Ismail, V. Fusco, D. Linton, N. Grant, and S. Rea, "Liquid crystal tunable mm wave frequency selective surface," *IEEE Microw. Wireless Compon. Lett.*, vol. 17, no. 9, pp. 667–669, Sep. 2007.
- [12] S. V. Hum and J. Perruisseau-Carrier, "Reconfigurable reflectarrays and array lenses for dynamic antenna beam control: A review," *IEEE Trans. Antennas Propag.*, vol. 62, no. 1, pp. 183–198, Jan. 2014.
- [13] S. H. Zainud-Deen, S. M. Gaber, and K. H. Awadalla, "Beam steering reflectarray using varactor diodes," in *Proc. Japan-Egypt Conf. Electron., Commun. Comput.*, Mar. 2012, pp. 178–181.
- [14] S. Foo, "Liquid-crystal reconfigurable, lens-enhanced, millimeter-wave phased array," *Inst. Eng. Technol.*, Stevenage, U.K., Tech. Rep. 318, 2018, p. 5.
- [15] C.-H. Zhao, Q. Wu, and F.-Y. Meng, "Design of reconfigurable circularly polarized reflectarray antenna at 100 GHz based on liquid crystals," in *Proc. Int. Conf. Microw. Millimeter Wave Technol.(ICMMT)* May 2019, pp. 1–4.
- [16] S. Foo, "Liquid-crystal reconfigurable metasurface reflectors," in *Proc. IEEE Int. Symp. Antennas Propag. USNC/URSI Nat. Radio Sci. Meeting*, Jul. 2017, pp. 2069–2070.
- [17] G. Perez-Palomino, M. Barba, J. A. Encinar, R. Cahill, R. Dickie, and P. Baine, "Liquid crystal based beam scanning reflectarrays and their potential in SATCOM antennas," in *Proc. 11th Eur. Conf. Antennas Propag. (EUCAP)*, Mar. 2017, pp. 3428–3431.
- [18] J. R. Reis, M. Vala, and R. F. S. Caldeirinha, "Review paper on transmitarray antennas," *IEEE Access*, vol. 7, pp. 94171–94188, 2019.
- [19] T. H. Cormen, C. E. Leiserson, R. L. Rivest, and C. Stein, *Introduction to Algorithms*, 3rd ed. Cambridge, MA, USA: MIT Press, 2009.
- [20] C. A. Balanis, *Antenna Theory: Analysis and Design*. Hoboken, NJ, USA: Wiley-Interscience, 2005.
- [21] M.-D. Zhu, T. K. Sarkar, and Y. Zhang, "Extrapolation of antenna near-field measurements using the iterative greedy algorithms," in *Proc. IEEE Int. Symp. Antennas Propag. USNC-URSI Radio Sci. Meeting*, Jul. 2019, pp. 2163–2164.



**EUIHO SHIN** (Student Member, IEEE) received the B.S. degree in electrical and computer engineering and industrial engineering from Seoul National University, South Korea, in 2020, where he is currently pursuing the M.S. degree. His current research interests include antenna design for 5G telecommunication and millimeter-wave radar systems.



**JUNGSEUK OH** (Senior Member, IEEE) received the B.S. and M.S. degrees from Seoul National University, South Korea, in 2002 and 2007, respectively, and the Ph.D. degree from the University of Michigan, Ann Arbor, USA, in 2012.

From 2007 to 2008, he was with Korea Telecom as a Hardware Research Engineer, working on the development of flexible RF devices. In 2012, he was a Postdoctoral Research Fellow with the Radiation Laboratory, University of Michigan. From 2013 to 2014, he was a Staff RF Engineer with Samsung Research America, Dallas, working as a Project Leader for the 5G/millimeter-wave antenna system. From 2015 to 2018, he was a Faculty Member with the Department of Electronic Engineering, Inha University, South Korea. He is currently an Assistant Professor with the School of Electrical and Computer Engineering, Seoul National University. He has published more than 40 technical journal and conference papers. His research interests include millimeter-wave (mmW) beam focusing/shaping techniques, antenna miniaturization for integrated systems, and radio propagation modeling for indoor scenarios. He was a recipient of the 2011 Rackham Predoctoral Fellowship Award from the University of Michigan. He has served as a Technical Reviewer for the IEEE TRANSACTIONS ON ANTENNAS AND PROPAGATION and the IEEE ANTENNA AND WIRELESS PROPAGATION LETTERS, among other journals. He has served as a TPC Member and the Session Chair for the IEEE AP-S/USNC-URSI and ISAP.

• • •